CO Oxidation on Pt: Variable Phasing of Inputs During Forced Composition Cycling

A combined experimental and theoretical investigation of the effect of forced feed composition cycling for CO oxidation on platinum has been performed. A novel approach to forced composition cycling was examined, in which the phase angle between the two input streams was varied. Reaction rate enhancement is shown to occur, and by varying the phasing of the feed streams it is possible to achieve a global maximum in the time-average reaction rate. This phenomenon can be explained quantitatively by a model based on an adsorbate-induced phase change of the Pt surface combined with CO adsorption self-exclusion. This mathematical model can also quantitatively describe the complex steady-state behavior (uniqueness-multiplicity transitions) observed for this reaction. The predictions of the model have been validated further through a detailed experimental study of the effects of feed flow rate, temperature, size of catalyst charge, and cycling frequency on the instantaneous and time-average conversions during forced cycling of the feed composition.

William R. C. Graham
David T. Lynch
Department of Chemical Engineering
University of Alberta
Edmonton, Alberta, Canada T6G 2G6

Introduction

Despite the apparent simplicity of the reaction, a complete mechanistic description of the CO oxidation on supported platinum has yet to be developed. This lack of knowledge is illustrated vividly by the variety of hypotheses proposed to explain the experimentally observed phenomena. For example, for the phenomenon of self-sustained oscillatory behavior it has been speculated that the oscillations could be due to: competitive adsorption of different types of surface CO (Hugo and Jakubith, 1972); coverage-dependent activation energies (Belyaev et al., 1974; Pikios and Luss, 1977); adsorption of inert (Eigenberger, 1978) or coreacting (Mukesh et al., 1982) species; variation of the catalyst surface temperature (Dagonnier et al., 1980; Jensen and Ray, 1982); kinetic nonlinearities in the reaction mechanism (Morton and Goodman, 1981); catalyst oxidation/reduction (Sales et al., 1982); variation of the oxygen sticking probability as a function of CO coverage (Ertl et al., 1982; Lynch et al., 1986); interaction of silicon impurities with the catalyst surface (Yeates et al., 1985); and diffusion of carbon to the catalyst surface (Burrows et al., 1987).

Several alternative hypotheses have been postulated even for the much less complex phenomenon of steady-state multiplicity. Hegedus et al. (1977) demonstrated that intrapellet diffusional resistances are important, while Chakrabarty et al. (1984) concluded that the interaction of the surface reaction with the adsorption/desorption processes, in the absence of diffusional limitations, is responsible for the multiplicities. Herskowitz and Kenney (1983) found that each of two quite different Langmuir-Hinshelwood-Hougen-Watson models could adequately predict the values of CO concentration at which transitions from low to high conversions occurred. Graham and Lynch (1987) showed that several very different models (standard Langmuir-Hinshelwood, oxidation-reduction, surface island, CO self-exclusion) could quantitatively describe the effect of operating conditions on the upper multiplicity boundary (transition from high to low conversion), but that only a model based on CO adsorption self-exclusion could describe the variations in the lower multiplicity boundary (transition from low to high conversions) over a wide range of CO and O_2 feed compositions. However, it was found that, even with quite extensive data, an essentially infinite number of different sets of parameter values could result in excellent agreement between the model predictions and the steady-state data.

As demonstrated by Kobayashi and Kobayashi (1974) and Bennett (1976), the use of transient response methods can often help to resolve questions concerning reaction mechanisms.

Correspondence concerning this paper should be addressed to D. T. Lynch.
W. R. C. Graham is currently with AECL Research Ltd., Chalk River, Ontario K0J 1J0.

These methods have often been used to examine CO oxidation on platinum, from which it has been determined that the bimolecular surface reaction between adsorbed species is the main reaction path at typically encountered reaction conditions (Engel and Ertl, 1979). Several investigations of CO oxidation have used a variant of the transient response method in which the feed composition is periodically manipulated, usually in the form of square wave cycles. As shown in modeling studies by Douglas and Rippin (1966) and by Bailey (1973), and in the seminal experimental study by Unni et al. (1973), the operation of catalytic reactors in a periodic manner can substantially improve the reaction rate and/or selectivity. In addition, periodic operation can be used to obtain insights into underlying reaction mechanisms. Cutlip (1979) found that forced composition cycling of the feed stream to a CSTR (continuous stirred tank reactor) resulted in reaction rate enhancement for CO oxidation on a supported platinum catalyst, and for this reaction Cutlip et al. (1983) and Graham and Lynch (1984) have shown that reaction rate enhancement can be partially explained by using models based on Langmuir-Hinshelwood-type mechanisms. Oh et al. (1978), however, have shown that a diffusion-reaction model, which accounts for surface accumulation, can adequately describe the rate enhancement that was observed when a tubular reactor was used. In a similar fashion, Cho (1983) found from a mathematical model of a single catalyst pellet that rate enhancement can be due to the interaction of diffusion with adsorption-desorption processes, whereas Barshad and Gulari (1985) believe that rate enhancement is due to an optimization of the amount of reactive CO surface species relative to nonreactive surface species.

In this investigation of CO oxidation on supported platinum, the effect of reactor operating parameters on rate enhancement during forced feed composition cycling is examined comprehensively for seven different sets of values of the mass of catalyst, the feed flow rate and the reactor temperature. In an earlier study (Graham and Lynch, 1987), the steady-state rate and multiplicity behavior were completely determined for each of these sets of reactor operating conditions. In this study, the effect of the frequency of the input cycle on the transient and time-average reaction rates is determined for each of the seven sets of operating conditions. In addition, a new mode of cyclical operation is examined in which the phase angle between inputs is varied. It is shown that the phase angle has a major effect on the time-average reaction rate. These data are used to evaluate a model combining the features of the surface phase transformation model that has been used to explain self-sustained oscillatory behavior (Lynch et al., 1986) and the CO self-exclusion model that has been used to account for steady-state multiplicity (Graham and Lynch, 1987). It is shown that the combined model is capable of quantitatively describing most of the experimental observations. Thus, this results in a single consistent explanation for three commonly observed complex phenomena: reaction rate resonance during feed composition cycling; steady-state multiplicity; and self-sustained oscillations that occur during CO oxidation on supported platinum.

Experimental Equipment and Materials

A 0.5 wt. % Pt/Al_2O_3 catalyst was used in an external recycle reactor system operated at 0.1 MPa total pressure for the reaction studies. From frequency response measurements similar to those described by Lynch and Walters (1990), the effective free volume of the reactor, bellows and associated tubing (excluding the volume of the catalyst and bed diluent) was determined to be 190 cm^3, and the mixing in the vessel was found to closely approximate that of an ideal CSTR. The details of the catalyst characteristics, experimental equipment and feed materials have been previously given by Graham and Lynch (1987), with the exception that modifications were made to the feed system to permit the generation of feed composition square waves as described by Graham and Lynch (1988). The CO and O_2 feed streams (specialty mixtures of CO/N_2 and O_2/N_2 from Linde) were each routed through air-actuated four-way valves, the timing of which was controlled with digital outputs from a HP minicomputer to achieve square wave cycling. Frequencies of up to 17 mHz were used in this study. This manner of generating square-wave composition cycles was found to be vastly superior to the alternative method of directly manipulating the flow controller setpoints. Steady-state and dynamic measurements of the CO_2 concentration in the reactor effluent were made using an infrared spectrophotometer set at 2,355 cm^{-1} which was interfaced to the minicomputer for real-time data accumulation and analysis.

Definition of oxygen phase lead

In this paper, the reactant feed composition was not maintained at a constant value. Instead, the feed concentration of each reactant was switched periodically between two values. During cycling, the CO feed mole fraction alternated between 2% for half of each cycle and 0% for the other half, with an average composition of 1%. The oxygen feed mole fraction alternated between 1% for half of each cycle and 0% for the other half, so that the average feed mole fraction of O_2 was 0.5%. Ultra-high-purity nitrogen (Linde) comprised the balance of the feed stream. Because the two four-way valves in the feed system could be independently manipulated, it was possible for the oxygen half-cycle to overlap with the CO half-cycle as much or as little as was desired. Different ways of cycling the reactants are shown in Figure 1. The overlap between the oxygen and CO half-cycles will be defined using the term "oxygen phase lead." Defining one complete feed cycle as having 360 degrees, the oxygen phase lead will refer to the fraction of a cycle, in degrees, between the start of an oxygen half-cycle (1% O_2) and the start of a carbon monoxide half-cycle (2% CO). Hence, as shown in Figure 1a, if the CO is switched off when the oxygen is switched on, and *vice versa,* an oxygen phase lead of 180 degrees results and the inputs are said to be out-of-phase. If the CO and O_2 are switched on and off simultaneously, as shown in Figure 1b, then the oxygen phase lead is zero degrees (or 360 degrees in-phase cycling). If the CO is turned on three-quarters of a cycle after the oxygen is turned on, as shown in Figure 1c, then the oxygen phase lead is 270 degrees, whereas if the CO is turned on after the oxygen has been flowing to the reactor for one-quarter of a cycle, as shown in Figure 1d, then the oxygen phase lead is 90 degrees. In general, any amount of oxygen phase lead is possible with the experimental equipment.

Experimental Behavior

The seven sets of reactor operating conditions used in this study, Table 1, are identical to those used previously by Graham and Lynch (1987), in which the steady-state rates and bifurcation behavior were determined for this system. The effects of

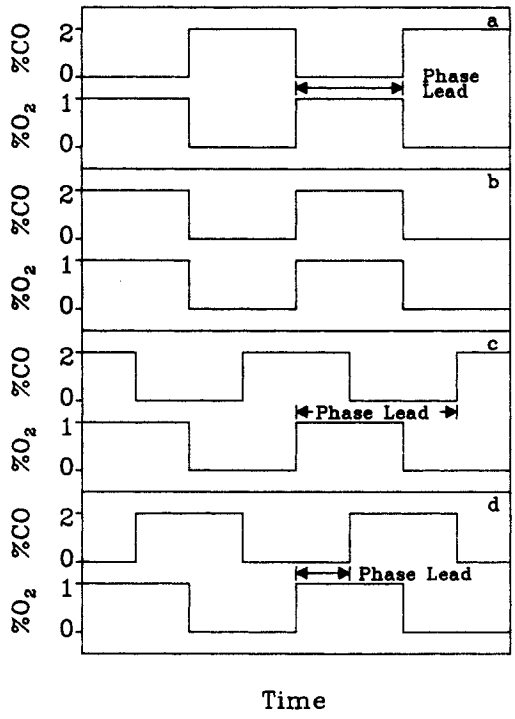

Figure 1. Feed cycling strategies.

Oxygen phase leads: a. 180 degrees; b. 0 degrees; c. 270 degrees; d. 90 degrees

operating conditions (mass of catalyst, temperature, and flow rate) on the multiplicity boundaries are summarized in Figure 2. In the cusp-shaped regions of Figure 2, multiple steady states exist. To the left of the multiplicity region only high-conversion steady states occur, while to the right of the multiplicity region only low-conversion steady states are present. Open symbols indicate the highest CO concentrations for which unique, high-conversion steady states were observed, whereas the solid symbols indicate the lowest CO concentrations for which unique, low-conversion steady states were found. The half-filled symbols mark the boundaries of the observed region of multiplicity. (A low-to-high conversion transition occurs at a concentration bracketed by an open and a half-filled symbol, whereas a high-to-low conversion transition occurs between each pair of half-filled and filled symbols.) See Graham and Lynch (1987) for additional information concerning the steady-state behavior for the seven sets of reactor operating conditions. The curves in Figure 2 are model predictions which will be described later.

In the first part of this study, the oxygen phase lead was maintained constant at 180 degrees, i.e., the inputs were

Table 1. Reactor Operating Conditions

Case	Mass of Cat. g	Temp. °C	Flow Rate mol/s
I	14.6	90	205×10^{-6}
II	4.95	90	68×10^{-6}
III	43.6	90	615×10^{-6}
IV	14.6	70	205×10^{-6}
V	14.6	110	205×10^{-6}
VI	14.6	90	68×10^{-6}
VII	14.6	90	615×10^{-6}

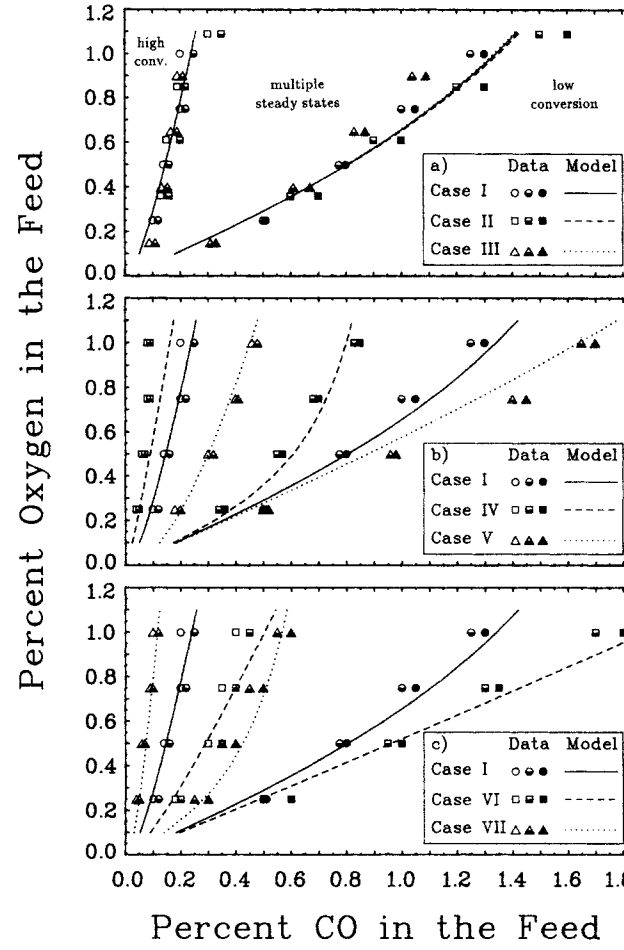

Figure 2. Steady-state bifurcation behavior.

a. Effect of mass of catalyst
b. Effect of temperature
c. Effect of flow rate (see Table 1 for operating parameters)

out-of-phase. The effects of size of catalyst charge, temperature, flow rate and frequency on the average conversion were examined. For out-of-phase feed switching, the (CO, O_2) feed composition alternates between (0%, 1%) for the first half-cycle and (2%, 0%) for the second half-cycle. The average feed composition of (1%, 0.5%) is in the unique low-conversion region in Figure 2 for all seven sets of operating conditions. For cycling in this manner, the feed alternates between the high and low conversion sides of the multiplicity region. A somewhat similar switching between the two sides of the multiplicity region occurs if the oxygen feed composition is held constant with only the CO feed composition cycled. This type of single-input cycling has been compared to 180-degrees out-of-phase cycling of the two feed streams by Graham and Lynch (1988), and it was found that both methods of feed cycling resulted in approximately equal time-average reaction rates. In the following, all feed cycling involved variation of both feed streams (CO and O_2 cycling).

In the second part of this study, the effect on the average conversion of the phase angle between inputs was examined for the base case (case I in Table 1) operating conditions. For cycling of this type the (CO, O_2) feed composition switched sequentially from (0%, 1%) to (2%, 1%), (2%, 0%), and (0%,

0%) for oxygen-phase leads between 0 and 180 degrees (see Figure 1d) and from (0%, 1%) to (0%, 0%), (2%, 0%), and (2%, 1%) for phase leads between 180 and 360 degrees (see Figure 1c). In every case an average feed composition of (1% CO, 0.5% O_2) was maintained.

Out-of-phase feed cycling

In the initial experiments, the reaction behavior during 180-degrees out-of-phase feed switching was determined. The dynamic CO_2 exit composition during out-of-phase cycling is shown in Figure 3 for case I operating conditions. At low frequencies (e.g., $\omega = 1.67$ mHz in Figure 3a) there are six distinct regions of interest during a single cycle. These regions are labeled in Figure 3a and are characterized as follows:

1. There is a rapid increase in CO_2 concentration as soon as the CO is switched on. At the start of this region, the catalyst surface is almost entirely covered with oxygen and the reactor oxygen composition is approximately 1%. During this period, almost all the CO entering the reactor adsorbs on the surface and reacts with adsorbed oxygen, which is being replenished from the gas phase. This period lasts until there is no gas-phase oxygen left in the reactor.

2. The rate of increase in CO_2 concentration decreases after the gas-phase oxygen has been depleted. During this interval, the CO entering the reactor adsorbs on the catalyst surface and cleans the surface of the remaining oxygen.

3. The CO_2 concentration falls as the reaction rate goes to zero. The gas-phase CO_2 concentration is not a direct indication of the reaction rate, because the alumina support has a large capacity for CO_2 adsorption-desorption. During this interval, the metal surface becomes saturated with CO.

4. When the CO feed is switched off and O_2 is switched on, the reaction rate does not immediately rise because the surface is almost entirely covered with CO, leaving very few pairs of empty sites for oxygen adsorption. The gas-phase CO concentration decrease is accompanied by a slow decrease in the surface coverage of CO due to both CO desorption and surface reaction processes.

5. When sufficient pairs of active sites become available for significant oxygen adsorption, there is a very sharp rise in the CO_2 concentration as most of the surface CO is eliminated by reaction with adsorbing oxygen.

6. In the final region, the remainder of the surface CO reacts to form CO_2, and the CO_2 concentration falls as the oxygen surface coverage increases. The desorption of CO_2 from the alumina support again (as in region 3) prevents the reactor CO_2 concentration from falling to zero.

As the frequency increases from that in Figure 3a, the peaks in the CO_2 concentration begin to merge and the different regions start to overlap or disappear. The double peak per cycle becomes a single peak per cycle, and, for high frequencies, the high-rate behavior disappears altogether. The time-average conversion for each cycling frequency is determined by integrating the area under the CO_2 concentration curve. Average conversions for the five cases in Figure 3, as well as for several additional frequencies, are shown in Figure 4, where, at very low frequencies, the time-average conversion increases almost linearly from zero. As the frequency increases, the time-average

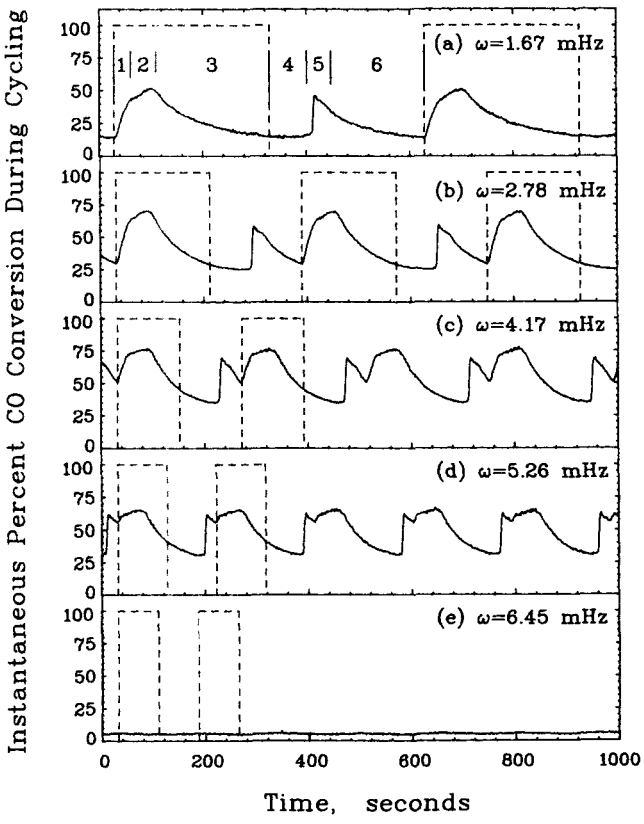

Figure 3. Instantaneous CO conversion during 180-degrees out-of-phase forced cycling: Case I data.

Dashed lines indicate the timing of step changes in the feed CO concentrations with oxygen step-changes 180 degrees out-of-phase

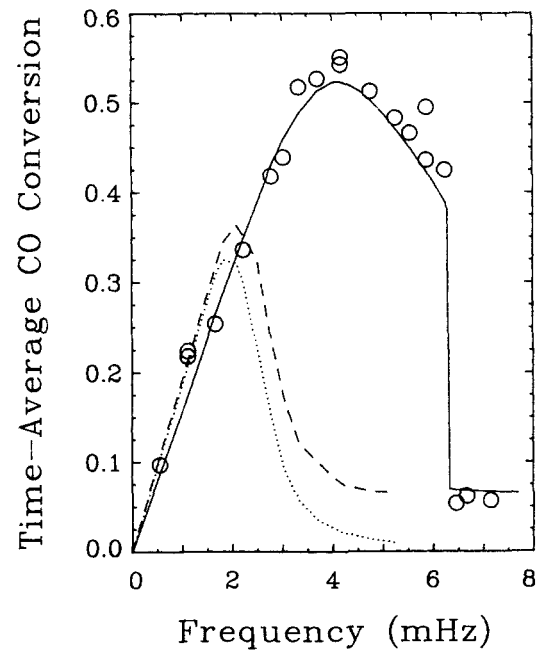

Figure 4. Predicted vs. experimental time-average conversions for 180-degrees out-of-phase forced cycling.

O, case I data; ·····, standard Langmuir-Hinshelwood model; - - - -, CO self-exclusion model; ———, Eqs. 4 to 10

conversion increases to a maximum and then decreases until a critical frequency is reached, following which the time-average conversion drops to a low value that approximately equals the steady-state conversion for a 1.0% CO and 0.5% O_2 feed. The curves in Figure 4 represent model predictions, which will be discussed later. Out-of-phase feed switching experiments were performed for several frequencies for each of the cases in Table 1, and the time-average conversions are summarized in Figure 5. For comparison, the base case (case I) results from Figure 4 are included in each of the panels of Figure 5.

Shown in Figure 5a is the effect of the mass of catalyst on the time-average conversion (with the ratio of feed flow rate to catalyst mass held constant). Although the steady-state bifurcation behavior was identical for cases I, II and III (see Figure 2a), the time-average behavior is quite different. Large catalyst charges lead to higher maximum average conversions during forced cycling, and the cycling frequency, at which the maximum average conversion occurs, increases with increasing catalyst mass. In Figure 5b it is seen that increasing temperature increases the maximum time-average conversion, while the data in Figure 5c show that decreasing the flow rate will increase the maximum time-average conversion.

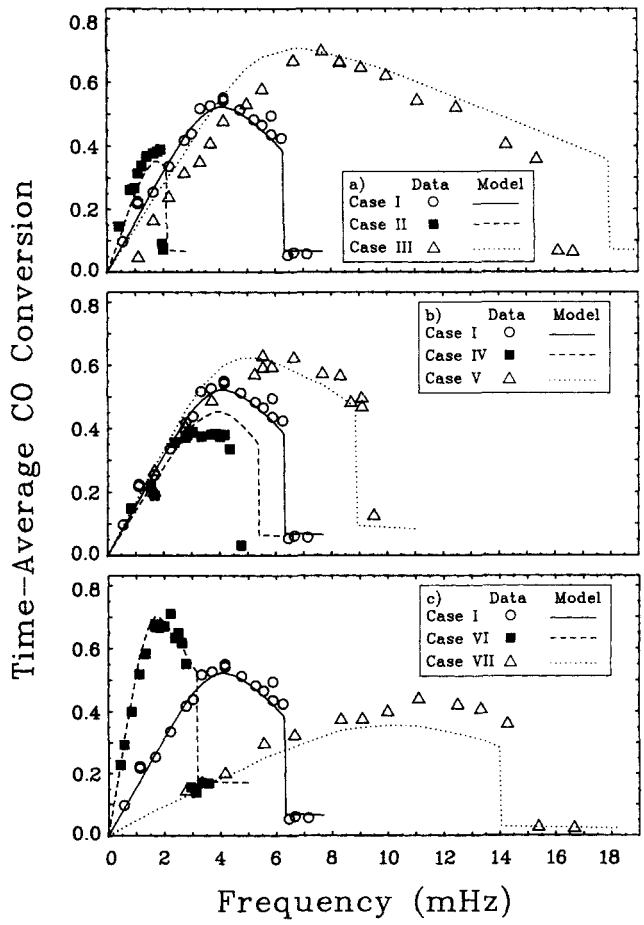

Figure 5. Effect of frequency on the time-average conversion during 180-degrees out-of-phase cycling.

Curves from Eqs. 4 to 10

a. Effect of mass of catalyst
b. Effect of temperature
c. Effect of flow rate (see Table 1 for operating parameters)

The critical frequency above which significant rate enhancement does not occur is determined primarily from mixing considerations and the steady-state bifurcation diagram (Figure 2). In the low-conversion steady-state region, the reaction rate does not significantly affect the reactant concentrations (conversion <10%, except for case VI). If it is assumed that the reactor concentration is not affected by the reaction, then for square-wave feed cycling to a CSTR the reactant concentrations will alternately increase and decrease in an exponential manner solely due to mixing effects. For a cycling frequency ω with switching between 0% and 2% CO in the feed, the extreme mole fractions of CO in the reactor will be

$$2\{1 + \exp[(-2\omega\tau_v)^{-1}]\}^{-1} \quad \text{and} \quad 2\{1 + \exp[(2\omega\tau_v)^{-1}]\}^{-1}$$

where $\tau_v = V/Q_o$. The reactor (CO, O_2) composition will remain on a line between (0%, 1%) and (2%, 0%) during cycling. As long as the reactor compositions stay to the right of the low-to-high-conversion bifurcation curve, the reactor will remain in a low-conversion state. If the reactor crosses to the left of the low-to-high-conversion bifurcation curve, the possibility of increased reaction rates will exist. To reach the high conversion branch of the rate curve, however, the surface must be cleaned of CO. The time required to clean the surface of CO will be approximately equal to $a_m L_m / f_{SS} Q_o [CO]_o$ (see the Notation section for the definition of symbols). If $F_{CO,crit}$ is defined as the CO composition (in percent) at the point where the line between (CO, O_2) compositions of (0%, 1%) and (2%, 0%) intersects the low-to-high-conversion bifurcation curve, then to a first approximation,

$$\omega_{crit} = \left[2\tau_v \ln\left(\frac{F_{CO,crit}}{2 - F_{CO,crit}}\right) + \frac{a_m L_m}{f_{SS} Q_o [CO]_o}\right]^{-1} \qquad (1)$$

For five of the seven cases in Table 1 (cases I–V), the observed critical frequency was within 15% of that predicted by Eq. 1. The largest difference was for case VI, where the predicted critical frequency was 55% higher than the experimental value (the steady-state conversion, f_{SS}, for case VI is not negligible, thus violating the stated assumptions). Thus, the critical frequency during out-of-phase cycling is strongly related to the time required for the concentrations to cross the low-to-high-conversion bifurcation boundary on the steady-state multiplicity diagram (Figure 2).

In the low-frequency regions of Figure 5, the frequency-conversion curve is linear. The slope is primarily a function of flow rate, reactor volume and catalyst surface area. For long cycle periods (low frequencies), the conversion will be limited by the amount of CO_2 produced by the alternate cleaning of the surface of adsorbed carbon monoxide and oxygen (the two peaks per cycle behavior shown in Figure 3a). The first peak, associated with switching on the CO feed, will contain an amount of CO_2 limited by the sum of one monolayer of oxygen on the catalyst surface and the gas-phase oxygen contained in the reactor volume. The second peak, which occurs after the oxygen feed is switched on, will contain an amount of CO_2 approximately equal to the CO in one surface monolayer (most of the gas-phase CO has left in the reactor effluent). The total CO_2 produced during the two peaks will thus be approximately equal to two monolayers plus twice (due to the stoichiometry) the feed oxygen concentration multiplied by the reactor volume. The

time-average conversion of a single cycle is defined as the total CO_2 production divided by the total amount of CO in the feed stream during a complete cycle. The CO in a single cycle is the product of the flow rate, the average feed concentration, and the period of the cycle. Thus, at low frequencies, the time-average conversion is approximately given by:

$$f_{TA} \approx \left(\frac{2a_mL_m + 2V[O_2]}{Q_o[CO]_o}\right)\omega \qquad (2)$$

Using experimentally determined values of $(f_{TA}Q_o[CO]_o/\omega)$ from the approximately linear portions of cases I to VII in Figure 5 and values of (a_mL_m) from hydrogen adsorption measurements, a linear regression was performed to obtain

$$f_{TA} = \left(\frac{0.92a_mL_m + 2.57V[O_2]}{Q_o[CO]_o}\right)\omega \qquad (3)$$

where the 95% confidence intervals for the constant terms are 0.92 ± 0.20 and 2.57 ± 0.83. The first constants in Eqs. 2 and 3 differ by more than a factor of two, but, considering the assumptions used to derive Eq. 2, the agreement between these equations is quite good. The $(2a_mL_m)$ term in Eq. 2 is an upper limit assuming that two complete monolayers react and that the number of catalytic sites for reaction is the same as for the hydrogen adsorption. If fewer than two monolayers react or if the number of active sites for reaction is less than that for hydrogen adsorption, then this term will be replaced by a smaller one. Herz and Marin (1980) summarized the data that oxygen uptakes are typically only about one-half the corresponding hydrogen uptakes, while Graham and Lynch (1987) explained that the ratio of adsorbed CO molecules to surface platinum atoms can be less than unity. Reduced uptakes of CO and oxygen relative to hydrogen would decrease the value of the contrast (2) in the first numerator term in Eq. 2. The second numerator term in Eq. 2 is based on the assumption that no gas-phase CO replenishes the surface after the oxygen feed is switched on. A small fraction of the gas-phase CO is more likely to adsorb on the surface after the introduction of oxygen, so this term should be larger than that given in Eq. 2.

From Eqs. 2 and 3, it is seen that large catalyst charges lead to large slopes, while large flow rates lead to small slopes. Thus, for operating conditions with the same flow rate and catalyst charge, the slope in the low-frequency region should be the same, even if the steady-state behavior is different. This was observed for reactor operation at different temperatures (cases I, IV and V) as shown in Figure 5b (same initial slope) and Figure 2b (different steady-state behavior).

The largest average conversion obtained during 180-degrees out-of-phase cycling was 71% for case VI with a frequency of 2.2 mHz. Although this is 4.5 times greater than the steady-state conversion for the same average feed composition, it is not greater than that which could be obtained from a combination of steady states with the same average feed composition. That is, this cycling strategy does not represent a global maximum. For example, by combining the exit streams from two steady-state reactors, one of which operates at a 100% conversion level with a (1.7% CO, 1% O_2) feed with the other operating at 0% conversion with a (0.3% CO, 0% O_2) feed with equal space times for both reactors, it is possible to obtain an average CO conversion of 85% while maintaining an overall combined (1% CO, 0.5% O_2) feed stream. This combination of two sets of steady-state operating conditions results in a higher average conversion than that obtained using 180-degrees out-of-phase cycling.

Effect of oxygen phase lead on time-average conversion

Following the completion of the first set of experiments, the effects of the phase angle between the feed square waves were determined. The phase-angle experiments were performed using the base case (case I) operating conditions. The time-average conversion is plotted against the oxygen phase lead for the five frequencies in Figure 6. (The solid lines represent model predictions which will be discussed later.) At frequencies higher than those shown in Figure 6 (e.g., for $\omega > 10$ mHz), the time-average conversion was always similar to that shown in Figure 6e for all values of the oxygen phase lead. As the cycle frequency was decreased, a small region of enhanced conversions appeared for oxygen phase leads of less than 180 degrees. For a period of 120 seconds, as shown in Figure 6d ($\omega = 8.33$ mHz), this region spans from 45 to 150 degrees. The maximum time-average conversion attained was greater than 90%, and this occurred for phase leads between 45 and 90 degrees. For phase leads less than 45 degrees or greater than 170 degrees, the

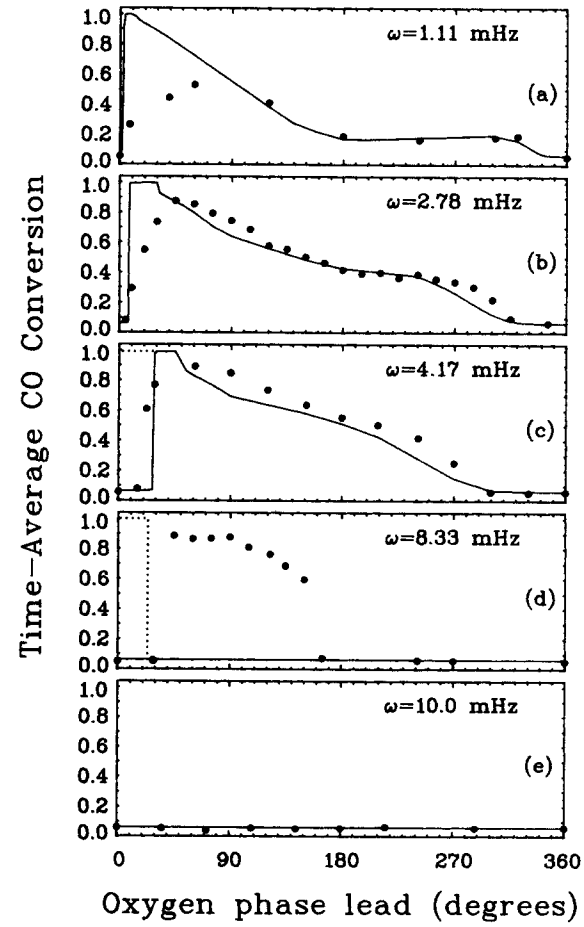

Figure 6. Effect of phase angle between CO and O_2 feed streams on the time-average conversion during forced cycling.

Curves from Eqs. 4 to 10

time-average conversion was approximately 5%. It is interesting to note that 180-degrees out-of-phase cycling does not lead to rate enhancement for this frequency (see case I in Figure 4 with $\omega = 8.33$ mHz).

As shown in Figure 6c for $\omega = 4.17$ mHz, the maximum time-average conversion is approximately 90%. This is greater than the largest time-average conversion (55% for case I conditions) obtained with 180-degrees out-of-phase cycling. Thus, by varying the phase angle between inputs, it is possible to improve the conversion obtained during feed composition cycling. The highest conversion attainable by combining the steady-state operating conditions of case I is 62.5% [one steady-state reactor with 100% conversion of a (1.25% CO, 1% O_2) feed and a second vessel with 0% conversion of a (0.75% CO, 0% O_2) feed stream]. Hence, with variable-phase cyclical operation it was possible to increase the maximum average reaction rate by more than 40%. This is an example of global rate enhancement.

As shown in Figure 6, as the frequency was decreased, the range of phase angles for which rate enhancement occurred increased, the maximum time-average conversion decreased, and a plateau region appeared for large oxygen phase leads. The plateau region is shown clearly in Figure 6a ($\omega = 1.11$ mHz) where it extends from about 180 to 320 degrees of oxygen phase lead (from 180 to 270 degrees for $\omega = 2.78$ mHz in Figure 6b). The plateau conversion is related to the catalyst charge, reactor volume, feed flow rate, and frequency in the same way as is the conversion in the low-frequency regions of Figure 5, and thus the plateau conversion can approximately be described by Eq. 3.

Despite a number of experimental studies of 180-degrees out-of-phase feed composition cycling, this is apparently the first—other than the preliminary study by Graham and Lynch (1988)—experimental report of the effect of phase angle variation during feed composition cycling. However, two somewhat limited mathematical studies of the effect of phase angle variation have been reported. Cho (1983) in his mathematical study of feed cycling to a single catalyst pellet, investigated only 0-, 90- and 180-degrees phase angles and the model predicted that the best performance should be achieved with 180-degrees out-of-phase cycling which is at odds with our findings. In an examination of an abstract catalytic model for parallel reactions, Zolotarskii et al. (1988) concluded that optimal performance was achieved when two input cycles overlapped to some extent, which is consistent with this study.

Model Details

The reaction was assumed to proceed via a Langmuir-Hinshelwood-type bimolecular surface reaction between reversibly adsorbed carbon monoxide and irreversibly adsorbed oxygen (dissociative adsorption). Two key assumptions made distinguish the mechanism from a standard LH mechanism. First, as described by Graham and Lynch (1987), it was assumed that CO self-exclusion occurs: on average, each adsorbed CO molecule prevents adsorption of further CO from slightly more than the one surface site occupied by the adsorbed CO molecule. Secondly, in a similar fashion to that described by Lynch et al. (1986), the catalyst surface was assumed to switch between two phases of different activity, as shown in Figure 7, when the critical values of CO surface coverage are reached.

As shown by Behm et al. (1983) and Thiel et al. (1983) for clean surfaces, the Pt(100) face reconstructs to a quasihexago-

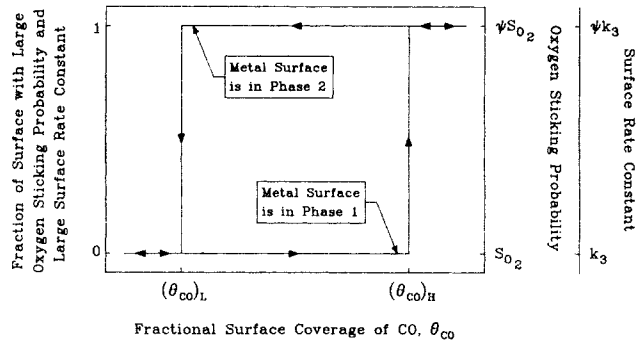

Figure 7. Effect of CO coverage on surface reaction and O_2 adsorption rate constants.

nal (hex) phase. This phase has a low sticking probability for oxygen adsorption. When the fractional surface coverage of CO exceeds a critical value, $(\theta_{CO})_H$, the entire surface spontaneously transforms to a (1×1) phase, i.e., the reconstruction is removed. The (1×1) phase has an oxygen sticking probability orders of magnitude higher than the hex phase. The metal surface remains in the (1×1) phase until the fractional surface coverage of CO drops below a second critical value, $(\theta_{CO})_L$. The surface then reconstructs to form the hex phase. These effects have been demonstrated using single crystals with well-defined faces. The applicability of these effects for supported-metal catalysts, such as that used in this study, has received support from the study by Wang et al. (1985) where it was shown that supported platinum crystallites form predominantly (100) crystal planes when grown in hydrogen.

In the mathematical representation of the surface phase-change phenomenon, the surface is considered to be a homogeneous surface, that is, the entire surface is either in phase 1 (hex) or phase 2 (1×1). In phase 1, the oxygen sticking probability and the surface reaction rate constant have low values, as shown in Figure 7. When the catalyst surface transforms to phase 2, the oxygen sticking probability and the surface reaction rate constant both increase by a factor of ψ, which for this work has been assigned a value of 250. When the surface transforms back to phase 1, the oxygen sticking probability and the surface reaction rate constant both return to their initial values. In Lynch et al. (1986), ψ was equal to 150 for the oxygen sticking probability and the surface reaction rate constant was assumed to be unaffected by the surface-phase transformation. In the initial attempts to fit the feed cycling data, the surface reaction rate constant was kept at the same value for both phases, but it was found that much better agreement with the data could be obtained by allowing the surface reaction rate constant to change in the same manner as the oxygen sticking probability.

When the preceding assumptions are incorporated into a mathematical model for an isothermal CSTR, the following equations result:

$$\frac{dX}{d\tau} = X_o - Q_n X - K_1 X(1 - \theta_{CO} - \theta_O) \cdot \frac{(1 - N_{CO}\theta_{CO})}{(1 - \theta_{CO})} + K_{-1}\theta_{CO} \quad (4)$$

$$\frac{dY}{d\tau} = Y_o - Q_n Y - K_2 Y(1 - \theta_{CO} - \theta_O)^2 \quad (5)$$

$$\frac{dZ}{d\tau} = Z_o - Q_n Z + K_3\theta_{CO}\theta_O - K_4 Z(1 - \phi_{CO_2}) + K_{-4}\phi_{CO_2} \quad (6)$$

$$\frac{d\theta_{CO}}{d\tau} = \alpha_m\left[K_1 X(1 - \theta_{CO} - \theta_O) \cdot \frac{(1 - N_{CO}\theta_{CO})}{(1 - \theta_{CO})} - K_{-1}\theta_{CO} - K_3\theta_{CO}\theta_O\right] \quad (7)$$

$$\frac{d\theta_O}{d\tau} = \alpha_m\left[\frac{2F_{O_2}}{F_{CO}} K_2 Y(1 - \theta_{CO} - \theta_O)^2 - K_3\theta_{CO}\theta_O\right] \quad (8)$$

$$\frac{d\phi_{CO_2}}{d\tau} = \alpha_s[K_4 Z(1 - \phi_{CO_2}) - K_{-4}\phi_{CO_2}] \quad (9)$$

where

$$Q_n = 1 - F_{CO}\left[K_1 X(1 - \theta_{CO} - \theta_O)\frac{(1 - N_{CO}\theta_{CO})}{(1 - \theta_{CO})} - K_{-1}\theta_{CO}\right] - F_{O_2}K_2 Y(1 - \theta_{CO} - \theta_O)^2 + F_{CO}K_3\theta_{CO}\theta_O - F_{CO}[K_4 Z(1 - \phi_{CO_2}) - K_{-4}\phi_{CO_2}] \quad (10)$$

These equations are identical to those used by Graham and Lynch (1987) except that in this model the rate constants for oxygen adsorption and surface reaction are given by:

$$K_2 = 6.43\, a_m \psi S_{O_2} \sqrt{T}/Q_o \quad (11)$$

$$K_3 = a_m L_m^2 \psi k_3 e^{-E_3/RT}/(Q_o[CO]_o) \quad (12)$$

where ψ is always unity for surface phase 1 (low CO coverage) and greater than unity for surface phase 2 (high CO coverage). This model reduces: to the CO self-exclusion model if ψ is always unity; to the surface-phase transformation model of Lynch et al. (1986) if $N_{CO} = 1$; and to the standard LH model if N_{CO} and ψ both are unity. For cycling of the type used in this study, X_o and Y_o both alternate between 0 and 2 (but not together unless the cycles are in phase), and Z_o is always zero because no CO_2 was present in the feed. Kinetic parameters for the model were chosen based on two criteria: the model should describe the steady-state bifurcation behavior (Figure 2); and the model predictions should match the experimental transient and time-average behavior (Figures 3 and 6) as closely as possible.

Model Predictions

First attempts at describing the time-average behavior used the standard LH model and the CO self-exclusion model with the rate parameters given by Graham and Lynch (1987), which minimized the error in the predicted steady-state bifurcation behavior. The predicted base case (case I) time-average conversions for these models are plotted in Figure 4. At low frequencies, the initial slope of the predicted conversion-frequency curve is approximately in agreement with the data. As previously mentioned, however, the slope of the initial linear region is determined by mass balance considerations. Thus, most kinetic models with correct values for volume, flow rate, and surface area will describe the slope, so the ability to predict the conversion in the low-frequency region is not an adequate test of a model. A better test is to examine the predicted behavior in the intermediate and high-frequency regions. As shown in Figure 4, neither the standard LH model nor the CO self-exclusion model could describe the time-average conversion for other than low frequencies. As frequency increases from low values, these models predicted a smooth transition to low time-average rates, unlike the data which showed an abrupt decrease in conversion at a critical frequency related to the location of the steady-state bifurcation boundary. Larger values of K_2 and K_3 are required if these models are to adequately describe the time-average behavior. However, increasing K_2 and K_3 causes the error in the predicted steady-state behavior to increase (agreement with steady-state behavior shown in Figure 2 must be maintained). The error in the predicted low-to-high-conversion bifurcation points can be reduced by increasing the ratio of K_1 to K_{-1}, but the error in the predicted high-to-low bifurcation points will remain unacceptable. If, however, K_2 and K_3 are increased only in the low-conversion, high-CO-coverage region, then it is possible to describe both the steady-state and the time-average behavior of the system. This is precisely what occurs when the surface-phase transformation model is used.

In the final modeling attempt, a value of ψ greater than unity was used, in this case $\psi = 250$. For the parameter values listed in the Notation section, the predicted steady-state behavior is shown in Figure 2. The model describes steady-state data very well. This is an important point of agreement between the model and the experimental data, as a model which does not correctly describe the observed steady-state behavior should not be used. The predicted case I time-average conversions are shown in Figure 4, where they are compared to the standard LH model and the CO self-exclusion model. The new model is superior to both of the existing models and quantitatively describes all of the major features of the conversion-frequency curve: the initial slope at low frequency, the magnitude and frequency of the maximum conversion, and the critical frequency after which significant rate enhancement does not occur. The model was also used to predict the effects of catalyst charge, temperature, and flow rate on time-average conversion. As shown in Figure 5, the resulting predictions are in excellent agreement with the data, describing all of the major features of the time-average conversion behavior.

The model predictions of the dynamic behavior during 180-degrees out-of-phase cycling are shown in Figure 8. Except for the CO_2 desorption preexponential factor, the parameters used for CO_2 adsorption and desorption on the support are identical to those used by Lynch et al. (1986). These predictions are for the conditions of case I. Each panel in Figure 8 can be compared directly with the corresponding panel in Figure 3. All of the important features of Figure 3 are also seen in Figure 8.

The final test of the model was to determine if it could describe the effect of oxygen phase lead on the time-average conversions. The predicted time-average conversion behavior is shown in Figure 6, where it is compared with the experimental results. At low and intermediate frequencies, as shown in Figures 6a to 6c, there is good agreement between the model predictions and the data with disagreement occurring only at low values of the oxygen phase lead where the model predicts

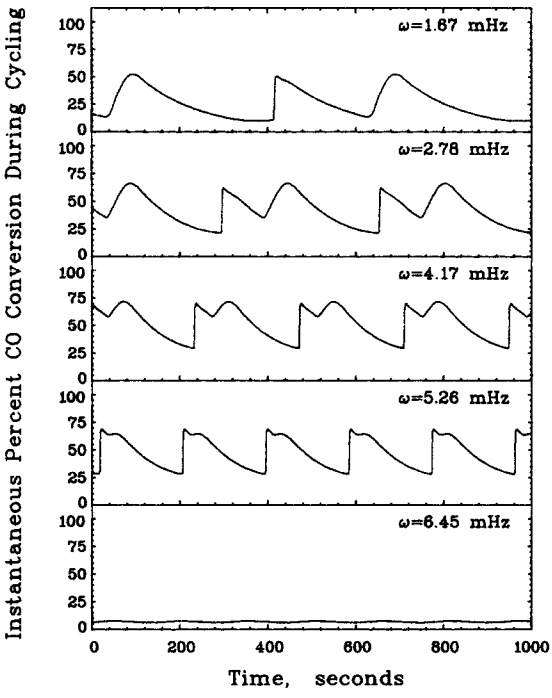

Figure 8. Predicted transient CO conversion for forced cycling.

Conditions as in Figure 3

higher CO conversions than were observed experimentally. The critical value of the phase lead at which the conversion drops from 100% to approximately 5% is affected by the initial conditions used when Eqs. 4 to 10 are integrated. The dotted curves in Figures 6c and 6d were obtained using initial conditions of zero for all of the integration variables, whereas the solid curves in Figure 6 were obtained with initial conditions of $X = 1$ and $\theta_{CO} = 0.995$ with all other variables set equal to zero. Because both cycling states are stable in the regions of overlap between the dotted and solid curves in Figure 6, the model predicts that a small region of multiplicity can exist for the time-average conversion depending on the chosen initial conditions. Outside of the overlap regions, the two sets of initial conditions produce identical time-average results and both are represented by the solid curves in Figure 6. The possible dependence of the time-average conversion on the initial reactor and surface conditions was not examined experimentally. All of the results presented in Figures 3 to 6 were obtained using a catalyst which was initially covered with CO, thus the experimental conditions were similar to that used to produce the solid curves in Figure 6.

There is another unusual prediction by the model: over certain small regions of phase lead, the model predicts that the time-average conversion can oscillate between several values, i.e., a "steady-state" cycling state is not reached. This was found to occur for several preliminary sets of parameter values that were examined when attempting to obtain agreement between the model predictions and the experimental observations. This is not surprising as it is well known that the forced cycling of a system, which can display multiplicity and oscillatory behavior, can result in diverse chaotic, multipeak and entrainment phenomena (Cordonier et al., 1990). This phenomenon was not observed experimentally; however, the model predictions indicate that it would be difficult to observe, because the predicted differences between the time-average conversions for successive cycles are not large.

The major disagreement between the model and the experimental observations is seen in Figure 6d where the model predicts (solid curve) that a low-conversion state will exist for all values of the oxygen phase lead, whereas experimentally a region of high time-average conversions was found. The model does predict that a small region of high time-average conversions is possible (dotted line) when initial conditions of zero are used for the integration of Eqs. 4 to 10; however, even in this case there is disagreement between the values of the phase lead over which high time-average conversions occur. This discrepancy could be due either to an incorrect choice of the parameter values or to the use of inappropriate assumptions in the model. For example, as shown by Ladas et al. (1989), the effect of subsurface oxygen on CO oxidation phenomena may be more important than surface reconstruction effects (particularly for Pd catalysts). Neither many alternative hypotheses [except as described by Graham and Lynch (1987) for the steady-state data] nor alternative sets of parameter values were exhaustively examined to eliminate this discrepancy, because, given the relative simplicity of this model, and the large amount of steady-state and dynamic data described here, the overall agreement between the model and the experimental data is quite good.

Conclusions

Four main conclusions can be drawn from this study of feed concentration cycling.

1. Rate enhancement occurs during forced feed composition cycling of the platinum-catalyzed CO oxidation reaction.

2. Variation of the phase angle between the oxygen and CO feed streams can cause increases in the time-average conversions over and above what occurs for out-of-phase cycling. The phase angle between inputs is an important parameter if maximum conversion is desired.

3. The standard Langmuir-Hinshelwood model, when forced to match the steady-state bifurcation behavior, is incapable of describing the observed rate enhancement during forced cycling.

4. A surface-phase transformation model with the CO self-exclusion can describe both the steady-state data and the rate enhancement for this system. A simplified form of this model (Lynch et al., 1986) has already been used to describe oscillatory behavior during CO oxidation; thus, the surface-phase transformation model with CO adsorption self-exclusion provides a single, consistent explanation for three of the commonly observed forms of complex behavior (steady-state multiplicity, self-sustained oscillations, and rate enhancement during forced cycling) exhibited by the CO oxidation on supported platinum catalysts.

Acknowledgment

The support of this research by the Natural Sciences and Engineering Research Council of Canada is gratefully acknowledged. W. R. C. Graham is grateful for the Province of Alberta Graduate Fellowship.

Notation

a_m = total surface area of the supported catalyst, 2.34 m^2 for 4.95 g charge, 6.92 m^2 for 14.6 g charge, 20.6 m^2 for 43.6 g charge

a_s = total surface area of the support, 1,600 m^2 for 14.6 g charge
[CO] = reactor and exit CO concentration, mol/m^3
$[CO]_o$ = time-average feed CO concentration, $F_{CO}P/RT$, mol/m^3
$[CO]_2$ = reactor and exit CO_2 concentration, mol/m^3
E_{-1}/R = activation energy for CO desorption, 13,900 K
E_3/R = activation energy for surface reaction, 5,800 K
E_{-4}/R = activation energy for CO_2 desorption from the support, 10,000 K
f_{SS} = steady-state conversion for a feed composition of 1% CO and 0.5% O_2
f_{TA} = time-average conversion of CO_2
F_{CO} = time-average fraction CO in feed
F_{O_2} = time-average fraction O_2 in feed
k_1 = CO adsorption rate constant, $6.87\, S_{CO}\sqrt{T}/L_m$, $m^3/mol \cdot s$
k^o_{-1} = CO desorption preexponential factor, $5 \times 10^{15}\ s^{-1}$
k_2 = O_2 adsorption rate constant, $6.43\, S_{O_2}\sqrt{T}/L_m^2$, $m^5/mol^2 \cdot s$
k^o_3 = surface reaction preexponential factor, $8.1 \times 10^{10}\ m^2/mol \cdot s$
k^o_{-4} = CO_2 desorption preexponential factor, $1.2 \times 10^{13}\ s^{-1}$
K_1 = dimensionless CO adsorption rate constant, $a_m L_m k_1/Q_o$
K_{-1} = dimensionless CO desorption rate constant, $a_m L_m k^o_{-1} \cdot \exp(-E_{-1}/RT)/Q_o[CO]_o$
K_2 = dimensionless O_2 adsorption rate constant, $a_m L_m^2 \psi k_2/Q_o$
K_3 = dimensionless surface reaction rate constant, $a_m L_m^2 \psi \cdot k^o_3 \exp(-E_3/RT)/Q_o[CO]_o$
K_4 = dimensionless CO_2 adsorption rate constant, $5.48\, a_s S_{CO_2} \cdot \sqrt{T}/Q_o$
K_{-4} = dimensionless CO_2 desorption rate constant, $a_s L_s k^o_{-4} \cdot \exp(-E_{-4}/RT)/Q_o[CO]_o$
L_m = adsorption capacity of the metal surface, $2 \times 10^{-5}\ mol/m^2$
L_s = CO_2 adsorption capacity of the support, $1.2 \times 10^{-6}\ mol/m^2$
N_{CO} = CO self-exclusion factor, 1.004
$[O_2]$ = reactor and exit O_2 concentration, mol/m^3
$[O_2]_o$ = time-average feed O_2 concentration, $F_{O_2}P/RT$, mol/m^3
P = reactor pressure, 0.1 MPa absolute
Q_n = ratio of exit to feed volumetric flow rates
Q_o = feed volumetric flow rate at reactor conditions, m^3/s
R = gas constant, $8.314\ m^3 \cdot Pa/mol \cdot K$
S_{CO} = CO sticking probability on catalyst, 1×10^{-3}
S_{O_2} = O_2 sticking probability on catalyst, 1.22×10^{-7}
S_{CO_2} = CO_2 sticking probability on support, 6×10^{-8}
t = time, s
T = reactor temperature, K
V = effective free volume of reactor, $1.9 \times 10^{-4}\ m^3$
X = dimensionless reactor CO concentration, $[CO]/[CO]_o$
X_o = instantaneous dimensionless feed CO concentration (0 or 2 in this study)
Y = dimensionless reactor O_2 concentration, $[O_2]/[O_2]_o$
Y_o = instantaneous dimensionless feed O_2 concentration (0 or 2 in this study)
Z = dimensionless reactor CO_2 concentration, $[CO_2]/[CO]_o$
Z_o = instantaneous dimensionless feed CO_2 concentration (0 in this study)

Greek letters

α_m = ratio of bulk volume to metal surface capacitances, $[CO]_o V/a_m L_m$ 0.455 for case I conditions
α_s = ratio of bulk volume to support surface capacitances, $[CO]_o V/a_s L_s$ 0.0328 for case I conditions
θ_{CO} = fractional CO surface coverage on the metal surface
$(\theta_{CO})_H$ = high critical value of θ_{CO} at which phase 1 to 2 transformation occurs, 0.95 in this study
$(\theta_{CO})_L$ = low critical value of θ_{CO} at which phase 2 to 1 transformation occurs, 0.10 in this study
θ_O = fractional oxygen surface coverage on the metal surface
τ = dimensionless time based on the reactor residence time, $Q_o t/V$
ϕ_{CO_2} = fractional CO_2 surface coverage on the support surface
ψ = enhancement factor for oxygen adsorption and surface reaction, 1 for surface phase 1, 250 for surface phase 2
ω = frequency of the forcing function, Hz

Literature Cited

Bailey, J. E., "Periodic Operation of Chemical Reactors: A Review," *Chem. Eng. Commun.*, **1,** 111 (1973).

Barshad, Y., and E. Gulari, "A Dynamic Study of CO Oxidation on Supported Platinum," *AIChE J.*, **31,** 649 (1985).

Behm, R. J., P. A. Thiel, P. R. Norton, and G. Ertl, "The Interaction of CO and Pt(100): I. Mechanism of Adsorption and Pt Phase Transition," *J. Chem. Phys.*, **78,** 7437 (1983).

Belyaev, V. D., M. M. Slin'ko, M. G. Slin'ko, and V. I. Timoshenko, "Autovibrations in the Heterogeneous Catalytic Reaction of Hydrogen and Oxygen," *Dokl. Akad. Nauk SSSR*, **214,** 1098 (1974).

Bennett, C. O., "The Transient Method and Elementary Steps in Heterogeneous Catalysis," *Catal. Rev.-Sci. Eng.*, **13,** 121 (1976).

Burrows, V. A., S. Sundaresan, Y. J. Chabal, and S. B. Christman, "Studies on Self-Sustained Reaction-Rate Oscillations: II. The Role of Carbon and Oxides in the Oscillatory Oxidation of Carbon Monoxide on Platinum," *Surface Sci.*, **180,** 110 (1987).

Chakrabarty, T., P. L. Silveston, and R. R. Hudgins, "Hysteresis Phenomena in CO Oxidation over Platinum-Alumina Catalyst," *Can. J. Chem. Eng.*, **62,** 651 (1984).

Cho, B. K., "Dynamic Behavior of a Single Catalyst Pellet: 1. Symmetric Concentration Cycling during CO Oxidation of Pt/Al_2O_3," *Ind. Eng. Chem. Fundam.*, **22,** 410 (1983).

Cordonier, G. A., L. D. Schmidt, and R. Aris, "Forced Oscillations of Chemical Reactors with Multiple Steady States," *Chem. Eng. Sci.*, **45,** 1659 (1990).

Cutlip, M. B., "Concentration Forcing of Catalytic Surface Rate Processes, Part 1. Isothermal Carbon Monoxide Oxidation Over Supported Platinum," *AIChE J.*, **25,** 502 (1979).

Cutlip, M. B., C. J. Hawkins, D. Mukesh, W. Morton, and C. N. Kenney, "Modelling of Forced Periodic Oscillations of Carbon Monoxide Oxidation over Platinum Catalyst," *Chem. Eng. Commun.*, **22,** 329 (1983).

Dagonnier, R., M. Dumont, and J. Nuyts, "Thermochemical Oscillations in Surface Reactions," *J. Catal.*, **66,** 130 (1980).

Douglas, J. M., and D. W. T. Rippin, "Unsteady State Process Operation," *Chem. Eng. Sci.*, **21,** 305 (1966).

Eigenberger, G., "Kinetic Instabilities in Heterogeneously Catalyzed Reactions—II. Oscillatory Instabilities with Langmuir-Type Kinetics," *Chem. Eng. Sci.*, **33,** 1263 (1978).

Engel, T., and G. Ertl, "Elementary Steps in the Catalytic Oxidation of Carbon Monoxide on Platinum Metals," *Adv. Catal.*, **28,** 1 (1979).

Ertl, G., P. R. Norton, and J. Rüstig, "Kinetic Oscillations in the Platinum-Catalyzed Oxidation of CO," *Phys. Rev. Lett.*, **49,** 177 (1982).

Graham, W. R. C., and D. T. Lynch, "Model Validation Through an Experimental Investigation of Resonant Behavior for the Catalytic Oxidation of Carbon Monoxide on Platinum," *Stud. Surface Sci. Catal.*, **19,** 197 (1984).

———, "CO Oxidation on Pt: Model Discrimination Using Experimental Bifurcation Behavior," *AIChE J.*, **33,** 792 (1987).

———, "Forced Cycling of Catalytic Reactors: Systems with Two Inputs," *Stud. Surface Sci. Cat.*, **38,** 693 (1988).

Hegedus, L. L., S. H. Oh, and K. Baron, "Multiple Steady States in an Isothermal, Integral Reactor: The Catalytic Oxidation of Carbon Monoxide over Platinum-Alumina," *AIChE J.*, **23,** 632 (1977).

Herskowitz, H., and C. N. Kenney, "CO Oxidation on Pt Supported Catalysts. Kinetics and Multiple Steady States," *Can. J. Chem. Eng.*, **61,** 194 (1983).

Hugo, P., and M. Jakubith, "Dynamisches Verhalten und Kinetik der Kohlenmonoxid-Oxidation am Platin-Katalysator," *Chem. Ing. Tech.*, **44,** 383 (1972).

Jensen, K. F., and W. H. Ray, "A Microscopic Model for Catalyst Surfaces—II. Supported Catalysts," *Chem. Eng. Sci.*, **37,** 1387 (1982).

Kobayashi, H., and M. Kobayashi, "Transient Response Method in Heterogeneous Catalysis," *Cat. Rev.-Sci. Eng.*, **10,** 139 (1974).

Herz, R. K., and S. P. Marin, "Surface Chemistry Models of Carbon Monoxide Oxidation on Supported Platinum Catalysts," *J. Catal.*, **65,** 281 (1980).

Ladas, S., R. Imbihl, and G. Ertl, "Kinetic Oscillations during the Catalytic CO Oxidation on Pd(110): The Role of Subsurface Oxygen," *Surface Sci.*, **219,** 88 (1989).

Lynch, D. T., "Modelling of Resonant Behavior during Forced Cycling of Catalytic Reactors," *Can. J. Chem. Eng.*, **61,** 183 (1983).

Lynch, D. T., G. Emig, and S. E. Wanke, "Oscillations during CO Oxidation over Supported Metal Catalysts: III. Mathematical Modeling of the Observed Phenomena," *J. Catal.*, **97,** 456 (1986).

Lynch, D. T., and N. P. Walters, "Frequency Response Characterization of Reaction Systems: External Recycle Reactor with a Solid Adsorbent," *Chem. Eng. Sci.*, **45**, 1089 (1990).

Morton, W., and M. G. Goodman, "Parametric Oscillations in Simple Catalytic Reaction Models," *Trans. Inst. Chem. Engrs.*, **59**, 253 (1981).

Mukesh, D., M. C. Cutlip, M. Goodman, C. N. Kenney, and W. Morton, "The Stability and Oscillations of Carbon Monoxide Oxidation over Supported Platinum Catalyst. Effect of Butene," *Chem. Eng. Sci.*, **37**, 1807 (1982).

Oh, S. H., K. Baron, J. C. Cavendish, and L. L. Hegedus, "Carbon Monoxide Oxidation in an Integral Reactor: Transient Response to Concentration Pulses in the Regime of Isothermal Multiplicities," *ACS Symp. Ser.*, **65**, 461 (1978).

Pikios, C., and D. Luss, "Isothermal Concentration Oscillations on Catalytic Surfaces," *Chem. Eng. Sci.*, **32**, 191 (1977).

Sales, B. C., J. E. Turner, and M. B. Maple, "Oscillatory Oxidation of CO over Pt, Pd and Ir Catalysts: Theory," *Surface Sci.*, **114**, 381 (1982).

Thiel, P. A., R. J. Behm, P. R. Norton, and G. Ertl, "The Interaction of CO and Pt(100): II. Energetic and Kinetic Parameters," *J. Chem. Phys.*, **78**, 7448 (1983).

Unni, M. P., R. R. Hudgins, and P. L. Silveston, "Influence of Cycling on the Rate of Oxidation of SO_2 over a Vanadia Catalyst," *Can. J. Chem. Eng.*, **51**, 623 (1973).

Wang, T., C. Lee, and L. D. Schmidt, "Shape and Orientation of Supported Pt Particles," *Surface Sci.*, **163**, 181 (1985).

Yeates, R. C., J. E. Turner, A. J. Gellman, and G. A. Somorjai, "The Oscillatory Behavior of the CO Oxidation Reaction at Atmospheric Pressure over Platinum Single Crystals: Surface Analysis and Pressure Dependent Mechanisms," *Surface Sci.*, **149**, 175 (1985).

Zolotarskii, I. A., S. M. Bogdashev, and Yu. Sh. Matros, "Efficiency of Catalytic Reactions with Periodic Concentration Oscillations of Two Reactants," *React. Kinet. Catal. Lett.*, **37**, 43 (1988).

Manuscript received July 19, 1990, and revision received Oct. 9, 1990.